JBC RESEARCH ARTICLE

N-glycosylation is a potent regulator of prion protein neurotoxicity

Received for publication, February 28, 2023, and in revised form, July 5, 2023 Published, Papers in Press, July 27, 2023,
https://doi.org/10.1016/j.jbc.2023.105101

Kevin M. Schilling[1], Pooja Jorwal[2], Natalia C. Ubilla-Rodriguez[1], Tufa E. Assafa[1], Jean R. P. Gatdula[2], Janelle S. Vultaggio[2], David A. Harris[2,*], and Glenn L. Millhauser[1,*]

From the [1]Department of Chemistry and Biochemistry, University of California, Santa Cruz, California, USA; [2]Department of Biochemistry, Chobanian & Avedisian School of Medicine, Boston University, Boston, Massachusetts, USA

Reviewed by members of the JBC Editorial Board. Edited by Joan B. Broderick

The C-terminal domain of the cellular prion protein (PrP^C) contains two N-linked glycosylation sites, the occupancy of which impacts disease pathology. In this study, we demonstrate that glycans at these sites are required to maintain an intramolecular interaction with the N-terminal domain, mediated through a previously identified copper–histidine tether, which suppresses the neurotoxic activity of PrP^C. NMR and electron paramagnetic resonance spectroscopy demonstrate that the glycans refine the structure of the protein's interdomain interaction. Using whole-cell patch-clamp electrophysiology, we further show that cultured cells expressing PrP molecules with mutated glycosylation sites display large, spontaneous inward currents, a correlate of PrP-induced neurotoxicity. Our findings establish a structural basis for the role of N-linked glycans in maintaining a nontoxic, physiological fold of PrP^C.

Prion diseases, or transmissible spongiform encephalopathies, are a class of fatal, infectious neurodegenerative illnesses caused by the refolding of the endogenous cellular prion protein (PrP^C) into a toxic isoform (PrP^{Sc}) (1, 2). These diseases, which are closely related to other protein aggregation disorders, including Alzheimer's and Parkinson's diseases, are a threat to cattle, cervids, and humans. Biosynthetically mature murine PrP^C is composed of 208 amino acids (residues 23–230) and is posttranslationally modified with a C-terminal glycophosphatidylinositol anchor and two Asn-linked glycans at residues 180 and 196. The N-terminal segment (residues 23–125, after removal of the signal peptide) exhibits a high degree of flexibility (3). Within this segment is an octapeptide repeat (OR) domain, residues 59 to 90, composed of the sequence $(PHGGXWGQ)_4$ in mouse PrP (where X is Gly in repeats one and four, Ser in repeats two and three), which binds the divalent ions Cu^{2+} and Zn^{2+} (4–7). The C-terminal domain (residues 126–230), which contains the glycan attachment sites, folds to a characteristic structure composed of three α-helices, numbered one through three, and two antiparallel β-strands flanking helix 1 (8, 9).

The N-terminal domain of PrP can interact with the lipid bilayer or with other membrane proteins to cause several toxic activities, including membrane leakage, spontaneous ionic currents, and neuronal death (10–14). It has been hypothesized that these activities may be responsible for the neurotoxic effects of prions during the disease process. The activity of the N-terminal, "toxic effector domain" is normally suppressed by an intramolecular interaction with the globular C-terminal domain (11, 15). Our research has demonstrated that copper binding to the OR segment promotes a stable contact between the two PrP domains that is essential for this regulatory interaction (11, 15, 16).

Extensive mutagenesis, combined with biophysical and electrophysiological experiments, provide a detailed structural picture of how the two domains of PrP interact (15). Specifically, copper drives the *cis* interdomain interaction through joint histidine coordination, in which His residues are contributed by each of the two domains (15). The C-terminal histidines (H139 and H176) are presented on a surface largely composed of α-helices 2 and 3 (Fig. 1). The N-terminal histidines are primarily those in the ORs. Conserved, C-terminal acidic residues (D177, E195, E199, E210), which lie on the same protein surface as the coordinating His residues, further facilitate this interaction. Familial mutations that reduce the negative charge of this patch have been linked to inherited prion diseases (17). These include the highly penetrant E200K mutation (E199K murine sequence), which causes Creutzfeldt–Jakob disease (CJD), and D178N (D177N murine), which causes fatal familial insomnia or CJD, depending on polymorphic residue 129 (M or V, respectively).

PrP^C's N-linked glycosylation sites are at asparagines 180 and 196, proximal to the location of many of its C-terminal pathological mutations (18). The protein exists *in vivo* as a mixture of unglycosylated, monoglycosylated, and diglycosylated forms. The glycans vary in their molecular composition and size. Glycosylation patterns vary between prion strains, which are characterized by differences in incubation time, neuropathology, and clinical symptoms (19–21). For example, the PrP^{Sc} found in two human prion diseases, familial CJD caused by V180I and variably protease-sensitive prionopathy, is devoid of glycosylation at N181 (22).

* For correspondence: David A. Harris, daharris@bu.edu; Glenn L. Millhauser, glennm@ucsc.edu.
Present address for Pooja Jorwal: McGovern Institute for Brain Research, MIT, Cambridge, Massachusetts, USA.

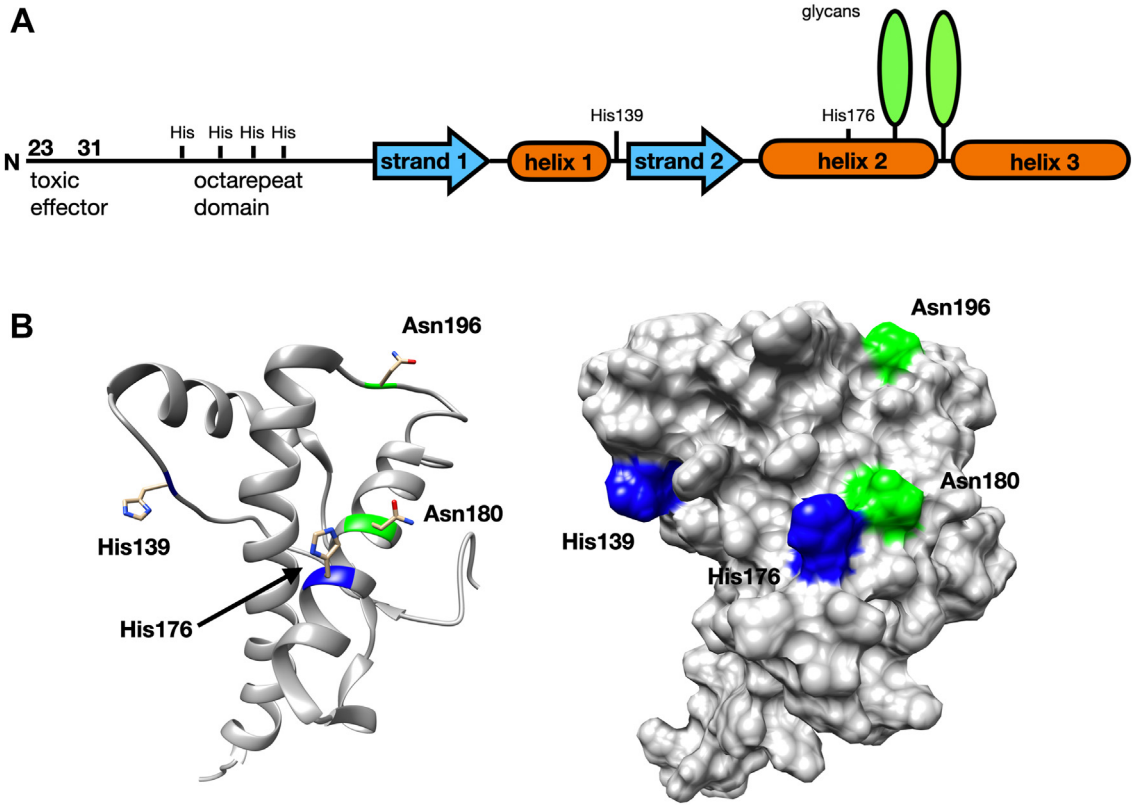

Figure 1. Structure of the prion protein indicating Asn glycosylation sites and regulatory histidine residues. *A*, linear diagram of the full-length PrP^{C}. *B*, ribbon and surface diagrams of the C-terminal domain of the prion protein. Note that the Asn-linked glycans are on the same C-terminal surface as the two histidines implicated in copper coordination. Graphics use Protein Data Bank: 1XYX.

Glycosylation also affects other properties of PrP^{C} and PrP^{Sc}. Glycosylation partially inhibits the aggregation of PrP^{C} into infectious PrP^{Sc}, decreasing its toxicity (23, 24). Glycosylation status also modulates cross-species transmission—the presence of a glycan at N196 prevents transmission of sporadic human CJD to mice (23). The presence of glycans also modulates the interaction between PrP^{C} and cofactors such as glycosaminoglycans (GAGs). GAGs accelerate prion disease by enhancing the conversion of PrP^{C} into PrP^{Sc} and promoting incorporation of PrP^{Sc} into plaques; glycans reduce PrP binding to GAGs (23, 25). The terminal saccharide in the prion protein's glycans is often sialic acid, which carries a negative charge at physiological pH. This may lead to electrostatic repulsion between copies of PrP, which could explain why sialylation slows the rate of PrP^{Sc} amplification (26–29). Prion strains show selective, strain-specific recruitment of PrP^{C} sialoglycoforms (30, 31). Lastly, the ratios of PrP^{C} glycoforms differ across brain regions, which may partially explain why prion strains have preferences for the regions that they infect (17, 32–34). In summary, the glycosylation status of the prion protein is intricately linked to many aspects of disease status, but the relationship is complicated and poorly understood.

The glycan linked to Asn180 is at a surface site near the middle of helix 2, while the glycan at Asn196 extends from a loop connecting helices 2 and 3 (Fig. 1). These sites are proximal to the C-terminal PrP^{C} surface containing the His residues that coordinate copper and are key to the *cis* regulatory interaction. Consequently, we deemed it essential to test whether glycosylation modulates C-terminal regulation of the N-terminal toxic effector domain. This is further motivated by the recognition that certain prion diseases produce PrP^{Sc} with no glycosylation at Asn180, a glycosylation site that is spatially adjacent by one helix turn from His176 (Fig. 1).

In this paper, we apply both electron paramagnetic resonance (EPR) and nuclear magnetic resonance (NMR) to artificially glycosylated, ^{15}N-labeled PrP^{C} to investigate the effects of the glycans on neuroprotective self-regulatory, *cis* interaction. Using EPR, we show that glycans on PrP^{C} do not significantly inhibit or alter its copper coordination environment. NMR experiments demonstrate that the glycans refine the *cis* interaction, localizing the copper interaction surface to a more focused area on the C terminus of the protein. Cell trafficking assays show that unglycosylated PrP^{C} is exported quantitatively to the cell surface. We showed previously that mutation of the C-terminal domain His residues impairs the observed *cis* interaction in unglycosylated PrP^{C}; new data presented here show that this impairment is reversed by glycosylation. Lastly, we find that unglycosylated PrP^{C} causes cultured cells to produce spontaneous inward cationic currents, a proxy for prion protein–induced toxicity. Surprisingly, the magnitude of these currents is similar to that observed for the highly toxic deletion mutant, ΔCR-PrP^{C}. Taken together, these results suggest that the glycans on the surface of the C-terminal domain of the prion protein participate in

maintaining a neuroprotective interdomain interaction, working in tandem with a previously discovered copper–histidine tether.

Results

Glycans on the C terminus of PrP^C do not significantly inhibit its copper binding

Bacterially expressed proteins lack glycans, while PrP from mammalian sources is heterogeneously glycosylated and cannot be easily isotopically labeled for structural studies. In order to create ^{15}N-labeled, homogenously glycosylated PrP in bacteria, we combined the genetic incorporation of the unnatural amino acid *p*-acetyl-phenylalanine with aminooxy-functionalized monosaccharides, coupling them together to form an oxime linkage, as described (35, 36). The monosaccharides were then enzymatically extended into trisaccharides using glycosyltransferases to yield the Sial-Gal-GlcNAc trisaccharide moiety (Fig. 2).

Continuous-wave EPR was used to probe the coordination environment of the copper bound to unglycosylated and artificially glycosylated PrP^C at pH 6.0. Experiments were performed with uniformly ^{15}N- (I = ½) labeled PrP^C, which gives better resolution of nitrogen superhyperfine coupling than protein containing the more abundant ^{14}N (I = 1) isotope. Samples contained 1:1 Cu^{2+}:protein, which favors so-called component 3 copper coordination, previously characterized as arising from interaction with three or four His imidazole side chains (37). Unglycosylated and glycosylated samples give nearly equivalent Cu^{2+} EPR spectra with no evidence of unbound, aquo copper (Fig. 3). The parallel regions of the spectra, between 2600G and 3100G, are an exact match with $g_{||}$ = 2.255 and $A_{||}$ = 570 MHz, as determined from simulations (Fig. 3). The values are consistent with component 3, multi-His coordination (37). The perpendicular regions match in multiplicity and field, with a slight difference in line broadening. Simulations show that these spectra are consistent with four equatorial nitrogen ligands (Fig. 3). We previously demonstrated that this coordination environment arises from three OR His residues and a His on the C-terminal regulatory surface (15). Overall, these data show that glycans on the C terminus of PrP^C do not inhibit or significantly alter its copper coordination modes.

Glycans on the C terminus of the prion protein refine its cis *interaction*

To evaluate the respective C-terminal interaction surfaces, we employed ^{1}H-^{15}N HSQC NMR analysis on glycosylated and unglycosylated PrP^C at pH 6. Divalent copper (d^9 electron configuration) possesses an unpaired electron that reduces the NMR signal intensity of nearby nuclei, in a distance-dependent manner, through paramagnetic relaxation enhancement. Intensities are measured from the 2D ^{1}H-^{15}N HSQC spectra and used to annotate residues on the PrP^C C-terminal domain. For clarity, only residues from 120 and beyond are displayed. Multiple representations of the data are shown in Figure 4. Figure 4, *A* and *B* are surface representations noting glycosylation sites (green) and with intensity reduction ranked as zero (gray), weak (light blue), and strong (navy blue). Figure 4, *C* and *D* show the same data plotted on a ribbon diagram. This representation shows clearly that all affected residues are located to helices 2 and 3, consistent with our previous findings. Figure 4, *E* and *F* provide position-dependent intensity ratios (i/i_o), allowing a quantitative comparison between the unglycosylated and glycosylated proteins.

We observed that the glycosylated prion protein displayed broadened signals on the C-terminal surface, like the unglycosylated protein, but that this broadening was concentrated to fewer residues and a smaller surface area (Fig. 4). Specifically, while the unglycosylated protein had significant line broadening around the areas of both His139 and His176, the

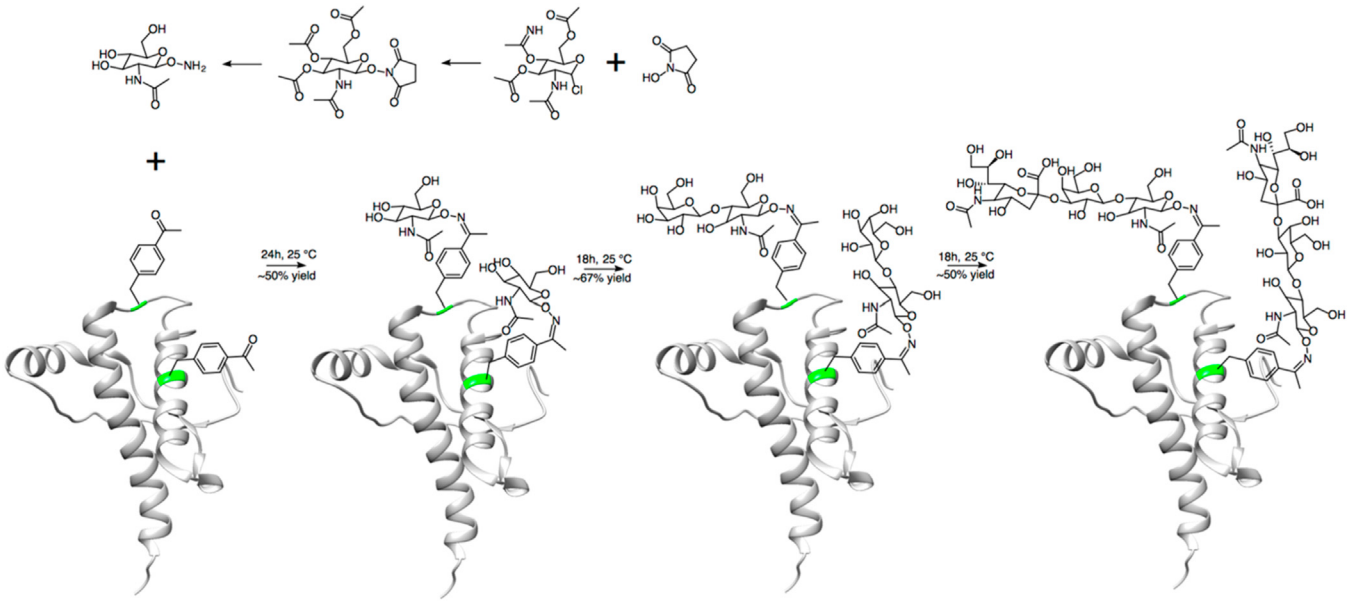

Figure 2. Synthesis scheme for glycosylated PrP. Plotted on Protein Data Bank: 1XYX. (Adapted from Schilling *et al. J. Org. Chem.* 85:1687–90, 2020.)

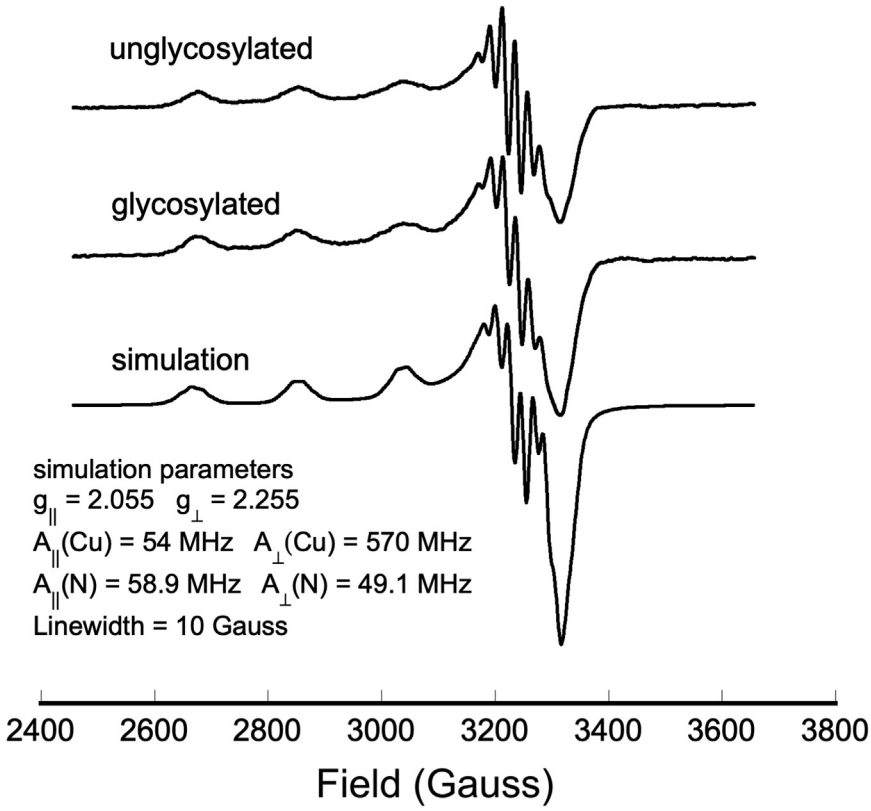

Figure 3. Continuous-wave EPR spectra of Cu^{2+} complexed with WT unglycosylated and artificially glycosylated PrP^C, along with a spectral simulation (parameters in the inset).

broadening in the glycosylated protein was focused mainly around histidine 176. This histidine is in close proximity to the glycan four residues (one helical turn) away, attached at position 180. This suggests that the glycans are not sterically hindering the *cis* interaction but, instead, are localizing the Cu^{2+}-OR segment to a more well-defined surface patch, primarily on helix 2.

Glycans partially restore cis *interaction lost by mutation of C-terminal histidines*

Histidines at positions 139 and 176 on the C-terminal domain of PrP^C coordinate copper together with N-terminal OR histidines, driving a neuroprotective, *cis* interaction through a metal ion molecular tether (15). We found previously that, when these C-terminal His residues are mutated to Tyr, the interaction is compromised, resulting in a much weaker interaction through a patch of negatively charged residues on the C-terminal surface (15). In addition, electrophysiological experiments performed on N2a cells expressing this mutant PrP^C lacking the C-terminal His residues showed weak spontaneous transmembrane currents, consistent with increased toxicity promoted by a poorly regulated N-terminal domain. By performing ^1H-^{15}N HSQC NMR analysis on both glycosylated and unglycosylated PrP^C(H139Y, H176Y) at pH 6, we found that the glycans largely restore the Cu^{2+}-promoted line broadening consistent with the interdomain *cis* interaction that is otherwise lost by elimination of the two His residues. Specifically, the unglycosylated wildtype protein has strong copper coordination around both histidines 139 and 176, whereas the glycosylated and histidine-mutated protein has strong copper coordination around the former location of histidine 176 only (Fig. 5). This suggests that the *cis* interaction in the cellular version of the protein may be exclusively between the N-terminal histidines and histidine 176 and is assisted by the nearby glycans.

Glycan elimination causes strong, spontaneous currents in cultured cells

Deletions in the central region of PrP, such as Δ105–125 (referred to as ΔCR), cause spontaneous, inward cationic currents in cultured cells and primary neurons (38, 39). Coexpression of wildtype PrP in cultured cells suppresses these currents, mirroring the ability of coexpressed wildtype PrP to suppress the neurotoxicity that accompanies these same mutations in transgenic mice (10). Antibodies that are neurotoxic when injected into the mouse brain also cause spontaneous currents in cultured cells (11). Therefore, the presence of spontaneous currents in cultured cells provides a surrogate readout of neurotoxicity caused by the prion protein. These currents are thought to be due to a weakening or abolishment of the neuroprotective *cis* interaction between the prion protein's N- and C-terminal domains, in turn allowing the polybasic N-terminal residues to form transmembrane pores (11, 40). Given our observation that glycans in the C-terminal domain enhanced the structural specificity of the *cis* interaction, we sought to test whether the absence of glycans

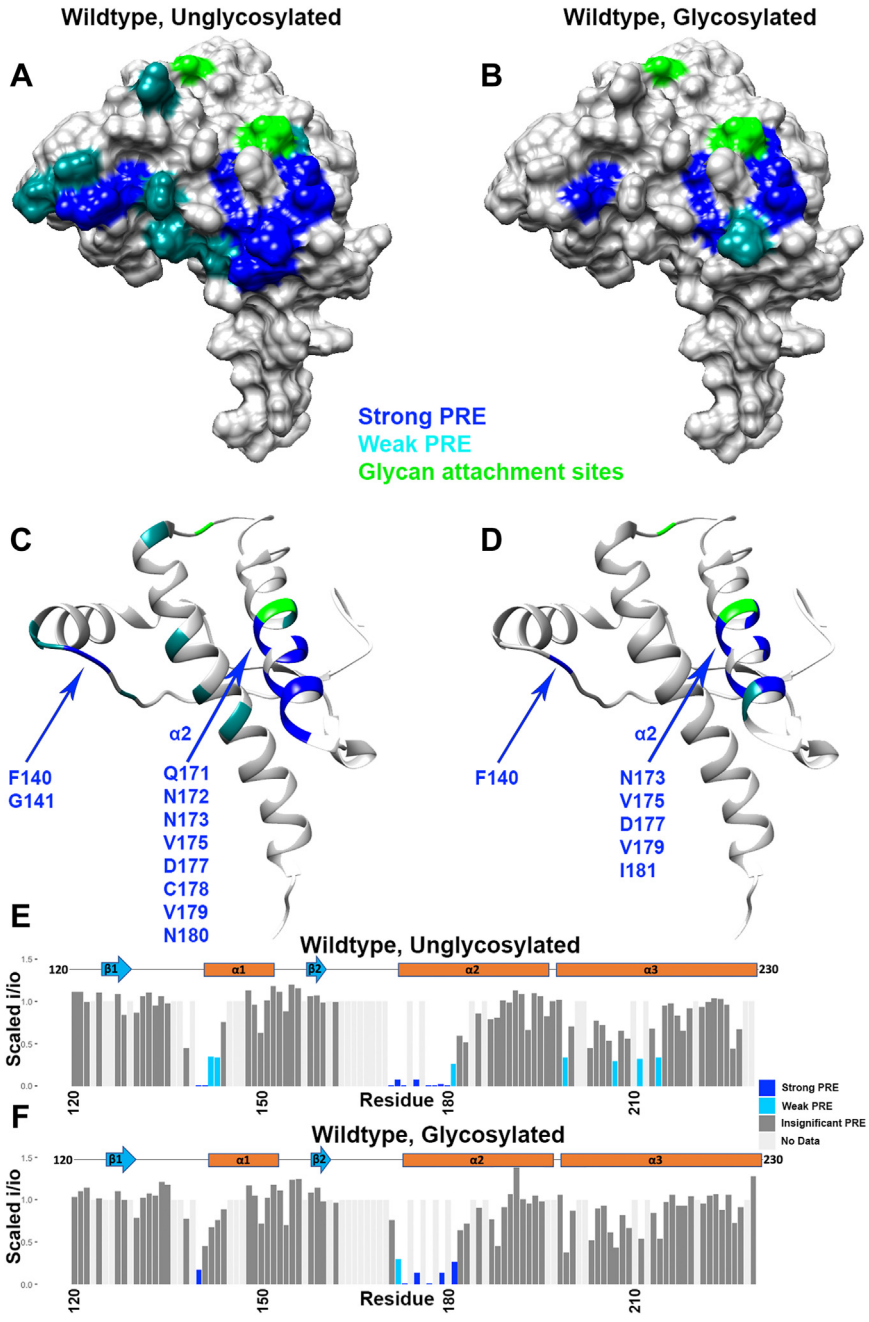

Figure 4. Influence of glycosylation on the PrP^C interdomain interaction. C-terminal residue lines are broadened due to PRE from N-terminally bound copper. Data were obtained from 2D ^{1}H-^{15}N HSQC NMR spectra; C-terminal residues shown here are annotated based on weak or strong PRE. Data are presented as (*A*) unglycosylated and (*B*) glycosylated surface representations, (*C and D*) ribbon plots, and (*E and F*) bar plots. Plotted on Protein Data Bank: 1XYX. PRE, paramagnetic relaxation enhancement.

perturbed the *cis* interaction, thereby causing spontaneous currents in cultured cells.

We created a PrP mutant, N180Q/N196Q, in which Asn residues at the two glycan attachment sites were changed to Gln residues, thereby preventing glycosylation at these sites but preserving the polar carboxamide side chain common to both Asn and Gln. In contrast to mutation of threonine residues in the N-X-T consensus sites, the N/Q mutations eliminate glycosylation but do not cause misfolding of PrP and do not alter its cellular trafficking or localization (41–44). To confirm the latter point, we expressed N180Q/N196Q PrP in N2a cells and used immunofluorescence staining to assess its cellular distribution. As shown in Figure 6, *A–C*, N180Q/N196Q PrP is localized to the cell surface, similar to WT PrP. Quantification of PrP cell surface expression is shown in Figure 6*D*. Western blotting confirmed similar overall PrP expression levels for all constructs and showed that elimination of both glycosylation sites results shifted the M_r of the expressed PrP to a lower M_r band corresponding to unglycosylated PrP (Fig. 6*E*).

Using whole-cell patch-clamp recording with holding potentials of either −70 mV or −90 mV, we observed

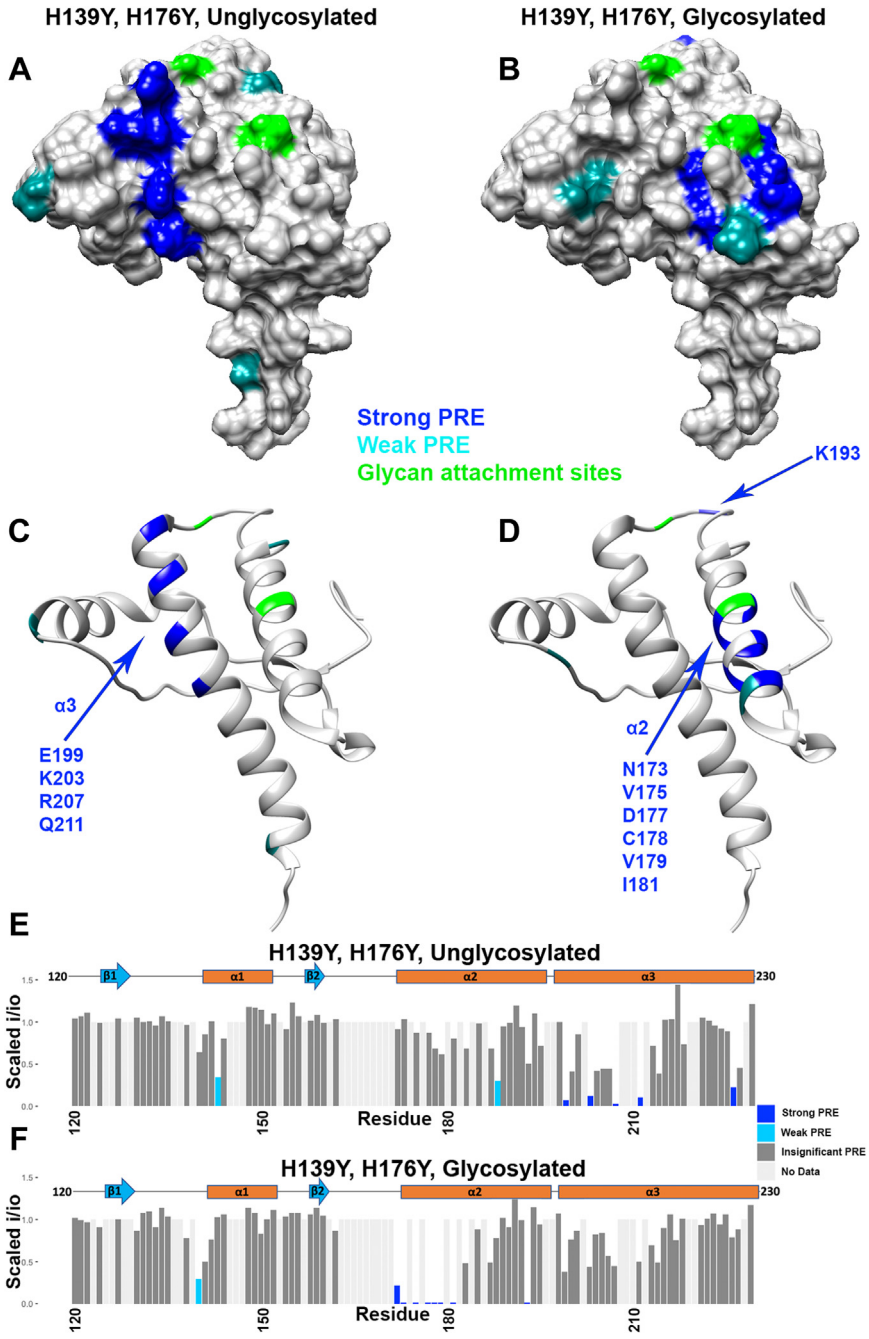

Figure 5. Influence of histidine mutation along with glycosylation on the PrP^C interdomain interaction. C-terminal residue lines are broadened due to PRE from N-terminally bound copper. Data were obtained from 2D ^1H-^{15}N HSQC NMR spectra obtained from PrP^C(H139Y, H176Y); C-terminal residues shown here are annotated based on weak or strong PRE. Data are presented as (*A*) unglycosylated and (*B*) glycosylated surface representations, (*C and D*) ribbon plots, and (*E and F*) bar plots. Plotted on Protein Data Bank: 1XYX. PRE, paramagnetic relaxation enhancement.

spontaneous inward currents for N180Q/N196Q PrP but not for the wildtype control (Figs. 7 and S1). We compared these currents to ΔCR PrP as a positive control and H139Y/H176Y PrP as a control that we previously showed produced currents at −90 mV but not at −70 mV (15). These data show that elimination of N-glycosylation causes strong spontaneous currents at −70 mV, quantitatively comparable with those observed for the highly toxic ΔCR PrP. Interestingly, we found little difference between N180Q/N196Q PrP, lacking the glycans, and the quadruple mutant N180Q/N196Q/H139Y/H176Y PrP, which lacks both glycans as well as the C-terminal His residues implicated in copper binding. Collectively, these data indicate that the C-terminal glycans play a significant role in stabilizing the interdomain *cis* interaction, thereby contributing to regulation of the toxic effector function of the N-terminal domain.

Discussion

In this study, we show that glycans on the C terminus of PrP^C refine the protein's neuroprotective, copper-driven *cis* interaction, localizing domain–domain contact to a well-

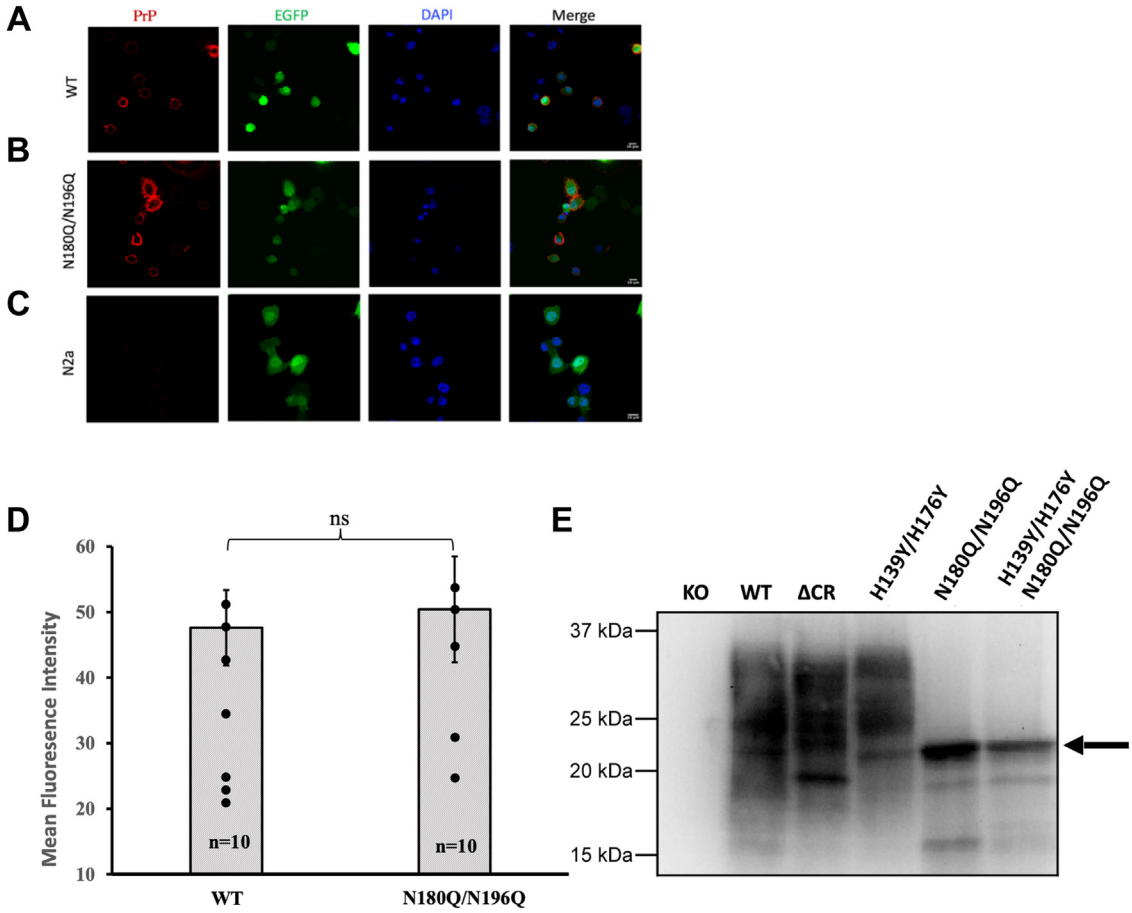

Figure 6. Expression of PrP constructs in N2a cells. *A–C*, N2a cells in which endogenous PrP expression was eliminated by gene editing were transfected with plasmids encoding WT PrP (*A*) or N180Q/N196Q PrP (*B*), along with an EGFP plasmid as a transfection marker. Cells in (*C*) were transfected with the EGFP plasmid alone. Cells were then fixed without permeabilization and immunostained for PrP using D18 antibody. Images show fluorescence for PrP, EGFP, DAPI, and a merge of all three channels. The results show that N180Q/N196Q PrP is present on the cell surface, similar to WT PrP. The scale bar represents 10 μm. *D*, quantification of cell surface expression of PrP on N2a cells transfected with WT and N180Q/N196Q PrP plasmids. Cell-surface fluorescence intensity for PrP was assessed in *A* and *B* using ImageJ software. Staining for PrP in C was undetectable. Bars show mean ± SE; n, number of cells used for quantitation. Cell surface expression of PrP was not significantly different between the two groups (ns). *E*, Western blot analysis of N2a PrP knockout cells transfected with vector alone (KO) or with plasmids encoding WT, ΔCR, H139Y/H176Y, N180Q/N196Q, and H139Y/H176Y/N180Q/N196Q PrP. The latter two constructs, which carry mutation of both glycosylation sites (N180Q and N196Q), show an unglycosylated band (*arrow*), as well as lower M_r bands corresponding to cleavage products.

defined region on the C-terminal domain. We further show that the presence of the glycans partially reverses loss of this interaction caused by the mutation of C-terminal histidines to tyrosines. Lastly, we find that unglycosylated PrP^C causes cultured cells to produce spontaneous inward currents, a readout that serves as a measure of PrP-induced neurotoxicity. Together, these results suggest that the glycans contribute structurally to autoregulation in the wildtype protein.

In a previous study, we found that two histidines on the C terminus of the prion protein drive a neuroprotective *cis* interdomain interaction by tethering the C terminus to an N-terminally bound copper ion. Here, we find that the PrP glycans also promote an N-C interaction, synergizing with the effect of His Cu coordination. A patch of negatively charged amino acids, located on the same protein surface as the histidines and glycans, is a third contributor (16, 45). More specifically, the cumulative data suggest that His176, acting through copper coordination, glycans at Asn180, and acidic residues D177, E195, E199, E210 act in concert to anchor the toxic effector N-terminal domain to its regulatory site on the C-terminal domain, as shown schematically in Figure 8.

Figure 8 summarizes a qualitative ranking among the various factors that control regulation of the N-terminal, toxic effector domain, as measured by the strength of the spontaneous currents induced by different mutants. Several familial forms of prion disease arise from mutations of acidic, C-terminal residues, including D177N and E199K (D178N and E200K in the human sequence). Previous work with the Zn^{2+}–PrP^C complex show that these mutations weaken the metal ion–promoted *cis* interaction. However, these mutations do not cause spontaneous currents in cultured cells. Next, we found that elimination of the C-terminal histidines, by His→Tyr mutagenesis, results in weak spontaneous currents that are observable only at hyperpolarizing transmembrane voltages of −90 mV. This effect is categorized as being "mildly toxic" (Fig. 8). Previous to this present study, extensive

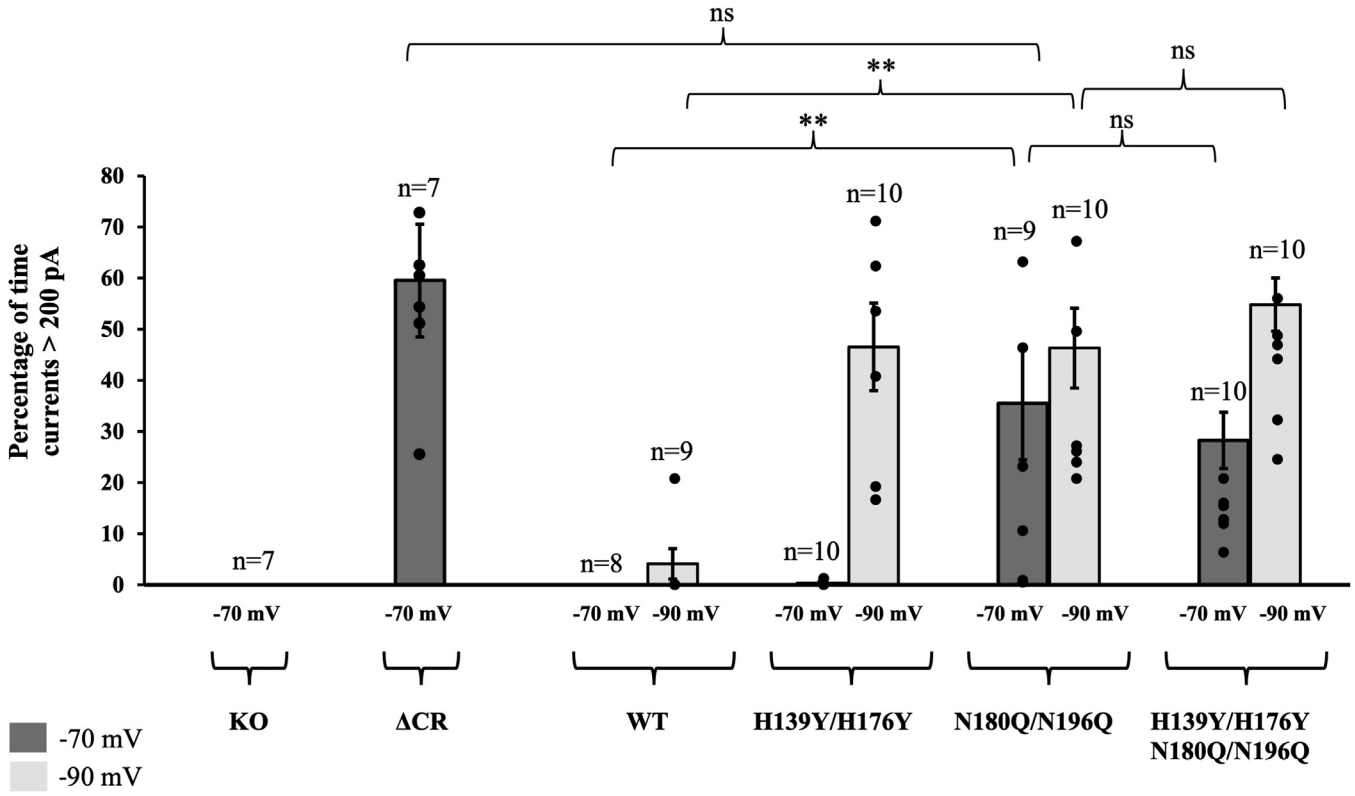

Figure 7. Whole-cell patch-clamp recordings from N2a cells expressing wildtype and relevant PrP^C mutants. Cells were untransfected (KO) or were transfected to express the following forms of PrP: Δ105–125 (ΔCR), wildtype (WT), H139Y/H176Y, N180Q/N196Q, and H139Y/H176Y/N180Q/N196Q. The holding potential was either −70 mV or −90 mV, as indicated. Bars show mean ± SEM. Each dot represents a recording from a single cell; n = number of cells. Differences are not significant (ns) or are significant with $p < 0.01$ (*double asterisk*). Mutation of both N-linked glycosylation sites (N180Q/N196Q) significantly enhanced spontaneous inward currents at a holding potential of −70 mV, even in the absence of mutation of the histidine residues (H139Y/H176Y).

investigations with the deletion mutant PrP^C(Δ105–125) (ΔCR PrP^C), which eliminates a portion of the linker between the toxic effector domain and the regulatory domain, revealed a significantly weakened *cis* interaction along with very strong spontaneous currents (11, 38, 39). Moreover, ΔCR PrP^C produces a neonatal lethal phenotype in Tg mice (10). Thus, we categorize this mutant as "toxic." In our previous studies, no other PrP mutant produced spontaneous currents as large as those observed for ΔCR PrP^C. Our present finding that the glycosylation mutant N180Q/N196Q produces such large, spontaneous currents is therefore unexpected and reveals a major role of N-linked glycans in regulating the toxic activity of the N-terminal domain.

How do the C-terminal glycans stabilize the interaction between the N- and C-terminal domains of PrP, and how does this effect synergize with that of copper coordination and binding to the acidic patch? In the absence of glycosylation, both C-terminal histidines (H139 and H176) contribute to copper coordination, as seen by enhanced paramagnetic relaxation enhancement at the two sites. However, with glycosylation, this interaction shifts preferentially to His176, which is one helical turn away from the glycosylation site at position 180. Thus, the additional glycan moiety at position 180 may provide an enhanced surface area for interaction with the hydrophobic OR domain. Alternatively, it is well established that protein glycosylation stabilizes protein–protein interactions through charge complementarity. For example, the tetrameric legume soybean agglutinin exhibits enhanced stability compared with other members of the same protein family by virtue of ionic contacts between its glycans and adjacent amino acid side chains (46). PrP^C possesses two polybasic charge clusters: one at the N terminus (residues 23–28) and the other between the OR and globular C-terminal domains (residues 100–109). The glycans terminate with negatively charged sialic acid residues, which may interact with these positively charged clusters, thereby stabilizing the folded state. In this case, loss of the glycan chains would destabilize the folded state, freeing the N-terminal domain to assume additional conformations.

Given the strong ionic currents induced by the double glycosylation mutant (N180Q/N196Q), which are similar to those induced by the highly pathogenic ΔCR mutant (Fig. 8), it might be predicted that expression of unglycosylated PrP in mice might produce a spontaneous neurodegenerative illness. Knockin mouse models expressing N180Q/N196Q PrP^C do exhibit greater susceptibility to plaque formation when inoculated with infectious prion strains; however, this study did not find evidence of neuronal dysfunction in uninoculated mice aged to 600 days (47). Other studies of transgenic mice expressing PrP glycosylation mutants examined the

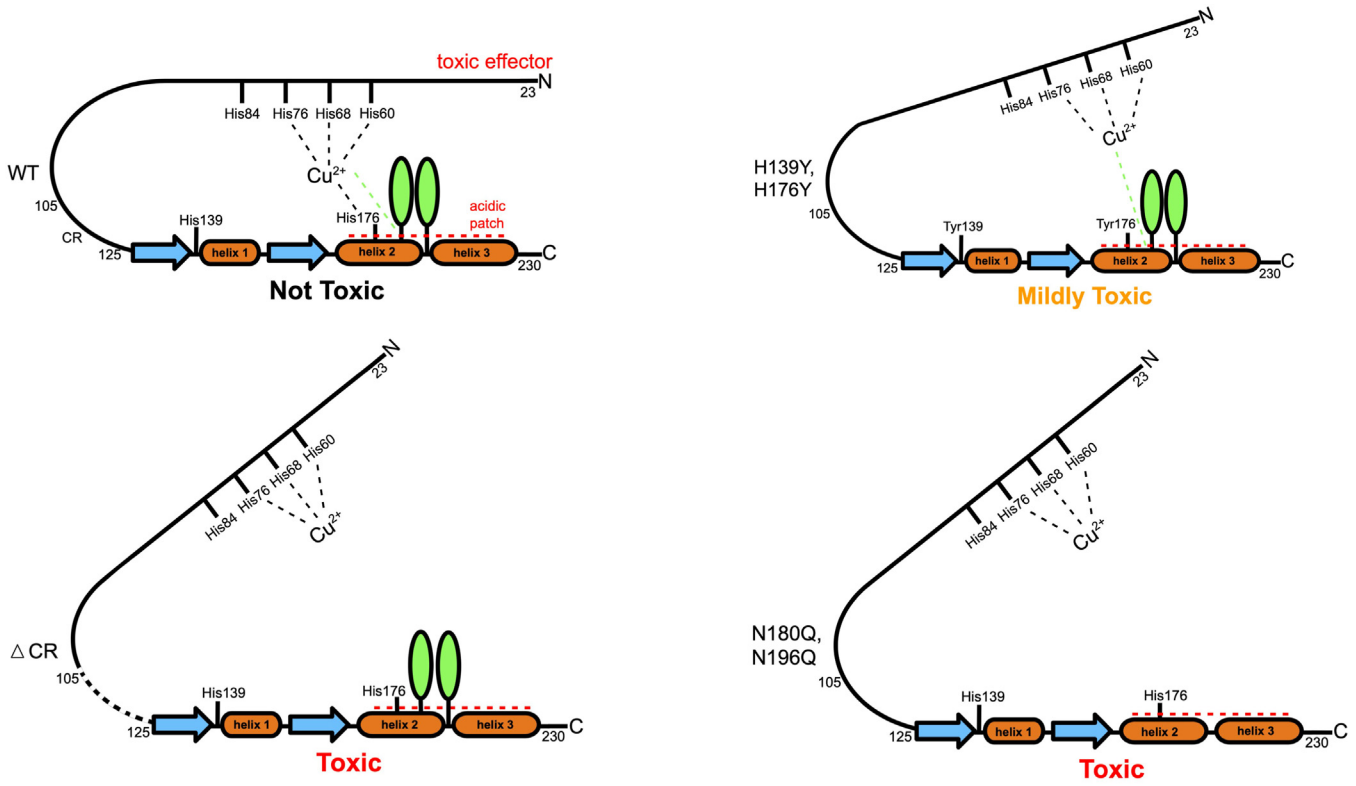

Figure 8. Unified model showing three contributors to the *cis* interaction in PrP^C. Displayed are the negatively charged patch produced by acidic residues in the C-terminal domain (*red dashed lines*), the Cu^{2+} coordinating to His residues in the OR and the regulatory C-terminal domain, and the glycans in the C-terminal domain (*light green ovals*). ΔCR PrP^C is the deletion mutant lacking residues 105 to 125.

consequences of Ala for Thr substitutions in the N-X-T consensus site (48, 49), mutations that are known to cause misfolding of PrP (41–43). These mice were analyzed for their susceptibility to prion infection, but no information was provided on the health of uninoculated mice.

PrP^C is normally found *in vivo* as a mixture of unglycosylated, monoglycosylated, and diglycosylated forms. Our observation that cells expressing the doubly deglycosylated mutant (N180Q/N196Q) display strong ionic currents raises the question of why the unglycosylated PrP normally found in the brain does not cause neuronal toxicity. However, it is also established that the potent neurotoxicity of PrP^C deletion mutants, such as Δ105–125 PrP^C, is ameliorated in multiple cell types and in transgenic mice when coexpressed with wildtype PrP^C (10, 38). We suggest that the coexpression of glycosylated PrP^C, or perhaps other PrP^C interactors in the brain, functions to suppress the inherent neurotoxicity of unglycosylated PrP^C.

Conclusions

This work identifies a fundamentally new protective role for glycosylation of PrP^C. Structurally, the C-terminal glycans help anchor and regulate interaction of the toxic, N-terminal effector domain with a regulatory surface on the C-terminal domain. Electrophysiological experiments demonstrated that lack of this glycan-mediated interaction leads to large transmembrane ionic currents, which could compromise cellular function. Thus, PrP^C glycosylation plays a crucial role in the structural and functional properties of PrP.

Experimental procedures

Protein preparation

The protein used for the experiments in this study was produced using a previously published protocol (36). Briefly, plasmids containing the genes for PrP and the necessary machinery to incorporate *p*-acetyl-phenylalanine were transformed into *E.coli*. The bacteria were grown in minimal media with ^{15}N ammonium chloride and *p*-acetyl-phenylalanine added, producing PrP with two *p*-acetyl-phenylalanine residues at the locations of the glycan attachment points. The protein was purified by nickel affinity chromatography and reverse-phase high-performance liquid chromatography (HPLC). The protein was allowed to react with aminooxy N-acetylglucosamine, which attached to the two *p*-acetyl-phenylalanines through oxime linkages. Glycosyltransferases were then used to extend these sugar into trisaccharides, and the protein was once again purified by HPLC. The resulting protein was glycosylated at both residues 180 and 196 with the trisaccharide N-acetylglucosamine, galactose, sialic acid.

Electron paramagnetic resonance spectroscopy

All samples were made to pH 6.0 in 50 mM 2-(*N*-morpholino)ethanesulfonic acid (Mes) buffer (Sigma), using potassium as a counterion. The protein was added to a

concentration of 100 μM, and $CuCl_2$ was used at 100 μM. The samples contained 30% glycerol as a cryoprotectant. X-band (9.38 GHz) continuous-wave EPR spectra were recorded on a Bruker EleXsys E580 spectrometer equipped with a super-high Q resonator (ER4122SHQE). Cryogenic temperatures were achieved with a liquid nitrogen finger Dewar and gas flow controller. The spectrometer settings were as follows: temperature = 121 K, conversion time = 41 ms, modulation amplitude = 0.5 mT, modulation frequency = 100 kHz, bridge power = 5 mW, attenuation = 23 dB.

Nuclear magnetic resonance spectroscopy

All samples were made to pH 6.0 in 10 mM 2-(*N*-morpholino)ethanesulfonic acid (Mes) buffer (Sigma), using potassium as a counterion and containing 10% D_2O. For all samples, the protein was added to a concentration of 100 μM. For samples with copper, $CuCl_2$ was used at 100 μM. ^{1}H-^{15}N HSQC spectra were recorded at 37 °C on a Bruker 800 MHz spectrometer at the UCSC NMR facility. NMR spectra were analyzed with NMR Pipe and Sparky using assignments transferred from previous experiments by visual inspection, and figures were made using Chimera, R, and python. To determine a cutoff i/i_0 value to separate the residues involved in the *cis* interaction from the rest of the protein, we performed a kernel density estimation on the data using a Gaussian smoothing kernel. To eliminate the effects of differential unspecific peak intensity reduction across mutants, the data were scaled so that the center values of each mutant's group of unaffected peaks were aligned. We divided the residues into three categories based on their i/i_0 values: strongly affected (dark blue), weakly affected (light blue), and unaffected (gray). These divisions were created by using the local minimum separating the affected from unaffected residues in the wildtype protein (i/i_0 = 0.35) and dividing the affected peaks into two groups (i/i_0 = 0–0.175 and i/i_0 = 0.175–0.35).

Cell culture

Mouse N2a cells (CCL-131, from the ATCC) were maintained in Opti-MEM Reduced Serum Medium (Thermo Fisher #31985088) supplemented with 10% (v/v) fetal bovine serum and 1% (v/v) penicillin/streptomycin (Thermo Fisher #15140122). Cells were maintained at 37 °C in a humidified incubator containing 5% CO_2 and were typically passaged every 4 days at a dilution of 1:5.

Generation of $PrP^{-/-}$ N2a cells

Ablation of endogenous PrP expression in N2a cells was done through CRISPR-Cas9 gene editing. N2a.$PrP^{-/-}$ clones were generated using a multiguide sgRNA system, followed by single cell cloning by limiting dilution. Briefly, three 1.5 nmol dry sgRNAs (Synthego), UCAGUCAUCAUGGCGAACCU, GGGCCAGCAGCCAGUAGCCA, and UCAUGGCGAACCUUGGCUAC were dissolved in 15 μl of nuclease-free 1× TE buffer to make a stock solution of 100 pmol/μl of sgRNA. This was pulse vortexed for 30 s and incubated at room temperature for 5 min to fully dissolve the sgRNA. A final concentration of 30 pmol/μl of the sgRNAs and 20 pmol/μl of a Cas9 2NLS nuclease (Synthego) were introduced to 1.0×10^6 cells through electroporation using Lonza's Amaxa Cell Line Nucleofector Kit V protocol (Program T-024). Cells were plated in six-well dishes for recovery. After 24 h or until 80 to 90% confluence, the cells were passaged into a T-75 flask (Fisher Scientific, # FB012937) for expansion. After 3 to 4 days or after confluence, N2a.$PrP^{-/-}$ cells were trypsinized, counted, and diluted to 2.0 cells/ml of medium, and 500 μl was plated in 48-well plates. The plates were monitored for 2 weeks for the presence of single-cell N2a.$PrP^{-/-}$ clones. Selected colonies were expanded sequentially in 12-well and then 6-well plates. N2a.$PrP^{-/-}$ clone candidates were analyzed and validated by Western blot analysis and using Synthego's Inference of CRISPR Edits (ICE) software. Clones that attained a knockout score of ≥ 90% in ICE and showed no trace of endogenous PrP^C expression on Western blots were selected and expanded further. A relatively fast-growing N2a.$PrP^{-/-}$ clone (Clone B5) was used for all experiments.

Whole-cell patch clamp experiments

N2a cells were maintained in Dulbecco's modified Eagle's medium supplemented with nonessential amino acids, 10% fetal bovine serum, and penicillin/streptomycin. Whole-cell patch-clamp recordings were taken from N2a cells 24 to 48 h after transient transfection, using Lipofectamine 2000, with pEGFP-N1 (Clontech) along with pcDNA3.1 vector encoding WT or mutant PrP. The N2a cells used here had been gene edited using CRISPR-Cas9 to disrupt the endogenous PrP gene. Recordings were done for 5-min durations using standard whole-cell patch-clamp technique (Fig. S1). Transfected cells were recognized by green florescence. Pipettes were pulled from thick-walled borosilicate glass filament with resistance 3 to 5 MΩ. Experiments were conducted at room temperature with an external recording solution containing 150 mM NaCl, 4 mM KCl, 2 mM $CaCl_2$, 2 mM $MgCl_2$, 10 mM glucose, and 10 mM Hepes (pH 7.4 with NaOH) and an internal recording solution containing 140 mM Cs-glucuronate, 5 mM CsCl, 4 mM MgATP, 1 mM Na_2GTP, 10 mM EGTA, and 10 mM Hepes (pH 7.4 with CsOH). Current signals were acquired using a Multiclamp 700B amplifier (Molecular Devices), digitized with a Digidata 1440 interface (Molecular Devices), and saved to disc for analysis with PClamp 10.7 software.

Immunofluorescence

About 24 to 48 h after transfection with EGFP, WT PrP, and mutant PrP plasmids, N2a cells were fixed with 4% paraformaldehyde in PBS and treated with 0.5% bovine serum albumin. PrP was detected using D18 antibody and Alexa Fluor 633–conjugated goat anti-human as secondary antibody, and nuclei were stained with DAPI. All images were acquired with a Zeiss LSM 700 confocal microscope under 63× magnification and analyzed using ImageJ. For quantification of PrP expression from immunofluorescence images, cells from each group (WT and N180Q/N196Q) were randomly selected for

statistical analysis after subtracting background fluorescence for each cell.

Western blotting

Protein samples were boiled in the presence of 1× Laemmli buffer (Bio-Rad) and loaded into 12% Criterion TGX Precast Protein Gels and run at 200 V for 35 min. Proteins were transferred to PVDF membranes for 45 min at 115 V before gentle washing in 0.1% TBST and blocking in 5% nonfat milk in 0.1% TBST for 1 h. Blots were treated with anti-PrP antibody D18 (50), followed by HRP-conjugated secondary antibody (Bio-Rad). Bands were visualized using ECL (Millipore).

Data availability

All processed data are contained within the article. Raw data, such as NMR spectra, are available from the corresponding authors.

Supporting information—This article contains supporting information.

Acknowledgments—We gratefully acknowledge NIH instrumentation grants S10OD018455 and S10OD024980 for acquisition of the 800 MHz NMR spectrometer and pulsed EPR spectrometer, respectively. We also thank Drs K. Sakamoto and S. Yokoyama at the RIKEN Yokohama branch, for providing the B-95.AAAfabR *E.coli* strain, and Amy Freiberg for help with the graphics.

Author contributions—K. M. S., D. A. H., and G. L. M. conceptualization; K. M. S., P. J., N. C. U.-R., T. E. A., J. R. P. G., and J. S. V. investigation; K. M. S., D. A. H., and G. L. M. writing – original draft; D. A. H. and G. L. M. writing – review & editing; D. A. H. and G. L. M. supervision.

Funding and additional information—We gratefully acknowledge NIH grants R35 GM131781 (to G. L. M.) and R01 NS065244 (to D. A. H.) for financial support. The content is solely the responsibility of the authors and does not necessarily represent the official views of the National Institutes of Health.

Conflict of interest—The authors declare that they have no conflicts of interest with the contents of this article.

Abbreviations—The abbreviations used are: CJD, Creutzfeldt–Jakob disease; EPR, electron paramagnetic resonance; GAG, glycosaminoglycan; OR, octapeptide repeat; PrP^{C}, cellular prion protein.

References

1. Prusiner, S. B. (1982) Novel proteinaceous infectious particles cause scrapie. *Science* **216**, 136–144
2. Prusiner, S. B. (1998) Prions. *Proc. Natl. Acad. Sci. U. S. A.* **95**, 13363–13383
3. Zahn, R. (2003) The octapeptide repeats in mammalian prion protein constitute a pH-dependent folding and aggregation site. *J. Mol. Biol.* **334**, 477–488
4. Aronoff-Spencer, E., Burns, C. S., Avdievich, N. I., Gerfen, G. J., Peisach, J., Antholine, W. E., *et al.* (2000) Identification of the Cu^{2+} binding sites in the N-terminal domain of the prion protein by EPR and CD spectroscopy. *Biochemistry* **39**, 13760–13771
5. Burns, C. S., Aronoff-Spencer, E., Legname, G., Prusiner, S. B., Antholine, W. E., Gerfen, G. J., *et al.* (2003) Copper coordination in the full-length, recombinant prion protein. *Biochemistry* **42**, 6794–6803
6. Millhauser, G. L. (2004) Copper binding in the prion protein. *Acc. Chem. Res.* **37**, 79–85
7. Millhauser, G. L. (2007) Copper and the prion protein: methods, structures, function, and disease. *Annu. Rev. Phys. Chem.* **58**, 299–320
8. James, T. L., Liu, H., Nikolai, B. U., Farr-Jones, S., Zhang, H., Donne, D. G., *et al.* (1997) Solution structure of a 142-residue recombinant prion protein corresponding to the infectious fragment of the scrapie isoform. *Proc. Natl. Acad. Sci. U. S. A.* **94**, 10086–10091
9. Riek, R., Hornemann, S., Wider, G., Billeter, M., Glockshuber, R., and Wuthrich, K. (1996) NMR structure of the mouse prion protein domain PrP(121-321). *Nature* **382**, 180–182
10. Li, A., Christensen, H. M., Stewart, L. R., Roth, K. A., Chiesa, R., and Harris, D. A. (2007) Neonatal lethality in transgenic mice expressing prion protein with a deletion of residues 105–125. *EMBO J.* **26**, 548–558
11. Wu, B., McDonald, A. J., Markham, K., Rich, C. B., and McHugh, K. P. (2017) The N-terminus of the prion protein is a toxic effector regulated by the C-terminus. *Elife* **6**, e23473
12. Sonati, T., Reimann, R. R., Falsig, J., Baral, P. K., O'Connor, T., Hornemann, S., *et al.* (2013) The toxicity of antiprion antibodies is mediated by the flexible tail of the prion protein. *Nature* **501**, 102–106
13. Chu, N. K., Shabbir, W., Bove-Fenderson, E., Araman, C., Lemmens-Gruber, R., Harris, D. A., *et al.* (2014) A C-terminal membrane anchor affects the interactions of prion proteins with lipid membranes. *J. Biol. Chem.* **289**, 30144–30160
14. Shmerling, D., Hegyi, I., Fischer, M., Blattler, T., Brandner, S., Gotz, J., *et al.* (1998) Expression of amino-terminally truncated PrP in the mouse leading to ataxia and specific cerebellar lesions. *Cell* **93**, 203–214
15. Schilling, K. M., Tao, L., Wu, B., Kiblen, J. T. M., Ubilla-Rodriguez, N. C., Pushie, M. J., *et al.* (2020) Both N-terminal and C-terminal histidine residues of the prion protein are essential for copper coordination and neuroprotective self-regulation. *J. Mol. Biol.* **432**, 4408–4425
16. Evans, E. G. B., Pushie, M. J., Markham, K. A., Lee, H.-W., and Millhauser, G. L. (2016) Interaction between prion protein's copper-bound octarepeat domain and a charged C-terminal pocket suggests a mechanism for N-terminal regulation. *Structure* **24**, 1057–1067
17. Minikel, E. (2013) *Prion Protein N-Linked Glycosylation: Review and Assessment of Therapeutic Potential*, CureFFI.org; Prion Alliance, Cambridge, MA
18. Rudd, P. M., Merry, A. H., Wormald, M. R., and Dwek, R. A. (2002) Glycosylation and prion protein. *Curr. Opin. Struct. Biol.* **12**, 578–586
19. Bessen, R. A., Kocisko, D. A., Raymond, G. J., Nandan, S., Lansbury, P. T., and Caughey, B. (1995) Non-genetic propagation of strain-specific properties of scrapie prion protein. *Nature* **375**, 698–700
20. Collinge, J., Sidle, K. C., Meads, J., Ironside, J., and Hill, A. F. (1996) Molecular analysis of prion strain variation and the aetiology of 'new variant' CJD. *Nature* **383**, 685–690
21. Piro, J. R., Harris, B. T., Nishina, K., Soto, C., Morales, R., Rees, J. R., *et al.* (2009) Prion protein glycosylation is not required for strain-specific neurotropism. *J. Virol.* **83**, 5321–5328
22. Xiao, X., Yuan, J., Haïk, S., Cali, I., Zhan, Y., Moudjou, M., *et al.* (2013) Glycoform-selective prion formation in sporadic and familial forms of prion disease. *PLoS One* **8**, e58786
23. Aguilar-Calvo, P., Callender, J. A., and Sigurdson, C. J. (2021) Short and sweet: how glycans impact prion conversion, cofactor interactions, and cross-species transmission. *PLoS Pathog.* **17**, e1009123
24. Yi, C.-W., Wang, L.-Q., Huang, J.-J., Pan, K., Chen, J., and Liang, Y. (2018) Glycosylation significantly inhibits the aggregation of human prion protein and decreases its cytotoxicity. *Sci. Rep.* **8**, 12603
25. Aguilar-Calvo, P., Sevillano, A. M., Bapat, J., Soldau, K., Sandoval, D. R., Altmeppen, H. C., *et al.* (2020) Shortening heparan sulfate chains prolongs survival and reduces parenchymal plaques in prion disease caused by mobile, ADAM10-cleaved prions. *Acta Neuropathol.* **139**, 527–546
26. Baskakov, I. V., Katorcha, E., and Makarava, N. (2018) Prion strain-specific structure and pathology: a view from the perspective of glycobiology. *Viruses* **10**, 723

27. Katorcha, E., Makarava, N., Savtchenko, R., d Azzo, A., and Baskakov, I. V. (2014) Sialylation of prion protein controls the rate of prion amplification, the cross-species barrier, the ratio of PrPSc glycoform and prion infectivity. *PLoS Pathog.* **10**, e1004366
28. Srivastava, S., Katorcha, E., Daus, M. L., Lasch, P., Beekes, M., and Baskakov, I. V. (2017) Sialylation controls prion fate *in vivo*. *J. Biol. Chem.* **292**, 2359–2368
29. Katorcha, E., Daus, M. L., Gonzalez-Montalban, N., Makarava, N., Lasch, P., Beekes, M., *et al.* (2016) Reversible off and on switching of prion infectivity via removing and reinstalling prion sialylation. *Sci. Rep.* **6**, 33119
30. Baskakov, I. V., and Katorcha, E. (2016) Multifaceted role of sialylation in prion diseases. *Front. Neurosci.* **10**, 358
31. Makarava, N., and Baskakov, I. V. (2022) Role of sialylation of N-linked glycans in prion pathogenesis. *Cell Tissue Res.* **392**, 201–214
32. DeArmond, S. J., Qiu, Y., Sànchez, H., Spilman, P. R., Ninchak-Casey, A., Alonso, D., *et al.* (1999) PrPc glycoform heterogeneity as a function of brain region: implications for selective targeting of neurons by prion strains. *J. Neuropathol. Exp. Neurol.* **58**, 1000–1009
33. Kuczius, T., Koch, R., Keyvani, K., Karch, H., Grassi, J., and Groschup, M. H. (2007) Regional and phenotype heterogeneity of cellular prion proteins in the human brain. *Eur. J. Neurosci.* **25**, 2649–2655
34. Somerville, R. A. (1999) Host and transmissible spongiform encephalopathy agent strain control glycosylation of PrP. *J. Gen. Virol.* **80**, 1865–1872
35. Liu, H., Wang, L., Brock, A., Wong, C.-H., and Schultz, P. G. (2003) A method for the generation of glycoprotein mimetics. *J. Am. Chem. Soc.* **125**, 1702–1703
36. Schilling, K. M., Ubilla-Rodriguez, N. C., Wells, C. W., and Millhauser, G. L. (2020) Production of artificially doubly glycosylated, 15N labeled prion protein for NMR studies using a pH-scanning volatile buffer system. *J. Org. Chem.* **85**, 1687–1690
37. Chattopadhyay, M., Walter, E. D., Newell, D. J., Jackson, P. J., Aronoff-Spencer, E., Peisach, J., *et al.* (2005) The octarepeat domain of the prion protein binds Cu(II) with three distinct coordination modes at pH 7.4. *J. Am. Chem. Soc.* **127**, 12647–12656
38. Solomon, I. H., Huettner, J. E., and Harris, D. A. (2010) Neurotoxic mutants of the prion protein induce spontaneous ionic currents in cultured cells. *J. Biol. Chem.* **285**, 26719–26726
39. Solomon, I. H., Khatri, N., Biasini, E., Massignan, T., Huettner, J. E., and Harris, D. A. (2011) An N-terminal polybasic domain and cell surface localization are required for mutant prion protein toxicity. *J. Biol. Chem.* **286**, 14724–14736
40. McDonald, A. J., Leon, D. R., Markham, K. A., Wu, B., Heckendorf, C. F., Schilling, K., *et al.* (2019) Altered domain structure of the prion protein caused by Cu2+ binding and functionally relevant mutations: analysis by cross-linking, MS/MS, and NMR. *Structure* **27**, 907–922.e905
41. Capellari, S., Zaidi, S. I., Long, A. C., Kwon, E. E., and Petersen, R. B. (2000) The Thr183Ala mutation, not the loss of the first glycosylation site, alters the physical properties of the prion protein. *J. Alzheimers Dis.* **2**, 27–35
42. Korth, C., Kaneko, K., and Prusiner, S. B. (2000) Expression of unglycosylated mutated prion protein facilitates PrP(Sc) formation in neuroblastoma cells infected with different prion strains. *J. Gen. Virol.* **81**, 2555–2563
43. Lehmann, S., and Harris, D. A. (1997) Blockade of glycosylation promotes acquisition of scrapie-like properties by the prion protein in cultured cells. *J. Biol. Chem.* **272**, 21479–21487
44. Linsenmeier, L., Mohammadi, B., Wetzel, S., Puig, B., Jackson, W. S., Hartmann, A., *et al.* (2018) Structural and mechanistic aspects influencing the ADAM10-mediated shedding of the prion protein. *Mol. Neurodegener.* **13**, 18
45. Spevacek, A. R., Evans, E. G. B., Miller, J. L., Meyer, H. C., Pelton, J. G., and Millhauser, G. L. (2013) Zinc drives a tertiary fold in the prion protein with familial disease mutation sites at the interface. *Structure* **21**, 236–246
46. Sinha, S., Mitra, N., Kumar, G., Bajaj, K., and Surolia, A. (2005) Unfolding studies on soybean agglutinin and concanavalin a tetramers: a comparative account. *Biophys. J.* **88**, 1300–1310
47. Sevillano, A. M., Aguilar-Calvo, P., Kurt, T. D., Lawrence, J. A., Soldau, K., Nam, T. H., *et al.* (2020) Prion protein glycans reduce intracerebral fibril formation and spongiosis in prion disease. *J. Clin. Invest.* **130**, 1350–1362
48. Neuendorf, E., Weber, A., Saalmueller, A., Schatzl, H., Reifenberg, K., Pfaff, E., *et al.* (2004) Glycosylation deficiency at either one of the two glycan attachment sites of cellular prion protein preserves susceptibility to bovine spongiform encephalopathy and scrapie infections. *J. Biol. Chem.* **279**, 53306–53316
49. DeArmond, S. J., Sanchez, H., Yehiely, F., Qiu, Y., Ninchak-Casey, A., Daggett, V., *et al.* (1997) Selective neuronal targeting in prion disease. *Neuron* **19**, 1337–1348
50. Safar, J. G., Scott, M., Monaghan, J., Deering, C., Didorenko, S., Vergara, J., *et al.* (2002) Measuring prions causing bovine spongiform encephalopathy or chronic wasting disease by immunoassays and transgenic mice. *Nat. Biotechnol.* **20**, 1147–1150